

Contents lists available at ScienceDirect

Cement and Concrete Composites

journal homepage: www.elsevier.com/locate/cemconcomp





Ascorbic acid: A green admixture for eco-efficient metakaolin blended cement with enhanced properties and corrosion resistance

Liang Wang ^{a,c}, Jialai Wang ^{b,*}, Hao Wang ^a, Xin Qian ^{b,d}, Yi Fang ^{b,e}, Yan Ge ^a, Xuepeng Wang ^a, Xiaozhi Zhao ^a, Monica Lages Do Amaral ^b

- ^a School of Civil Engineering and Architecture, Anhui University of Science and Technology, Huainan, Anhui 232001, PR China
- b Department of Civil, Construction, and Environmental Engineering, The University of Alabama, Tuscaloosa, AL, 35487, USA
- ^c Huaibei Mining Co. Ltd., Huaibei, Anhui 235000, PR China
- d Key Laboratory of Infrastructure Durability and Operation Safety in Airfield of CAAC, Tongji University, Shanghai 201804, PR China
- ^e College of Mechanics and Materials, Hohai University, Nanjing, Jiangsu, 211100, PR China

ARTICLE INFO

Keywords: Ascorbic acid Multipurpose admixture Metakaolin Compressive strength Corrosion inhibition

ABSTRACT

This study explores ascorbic acid (AA) as a green, multipurpose admixture to improve the eco-efficiency of metakaolin (MK) blended cement mortar. The AA can be simply added into a mortar mix at a very small dosage to function as a hydration retarder, a water reducer, a strength enhancer, an autogenous shrinkage reducer, and a corrosion inhibitor for reinforcing bars. With four hydroxyl groups, AA can be adsorbed on the surface of cement particles, leading to slower hydration rate of cement and better dispersion of its hydration products. Both the porosity and small capillary pores of mortar are drastically reduced by the addition of AA. This leads to not only significant increase of compressive strength of MK blended cement mortar, but also significant reduction in the autogenous shrinkage. An accelerated corrosion test validated the corrosion resistance of reinforcing bar embedded in mortar by adding AA. This study broadens the range of molecules and polymers for interaction with cement and provides a new pathway for developing next the generation of chemical admixtures for concretes.

1. Introduction

Concrete with Ordinary Portland cement (OPC) as the binder is the most used construction material. The production of OPC is a CO_2 and energy-intensive process as the cement industry alone emitted around $2.3 \times 10^9 \, \mathrm{m}^3$ tons of carbon dioxide (CO₂) in 2019 [1]. An effective strategy to decarbonize concrete is to substitute some OPC with low-carbon supplementary cementitious materials (SCMs) [2] such as Metakaolin (MK) [3]. Unlike the production of OPC clinker, production of MK is a process of dehydroxylation without CO_2 release. The heat required for MK production only releases 175 kg of CO_2 for one ton of MK, less than one-fifth of the CO_2 emissions generated by producing the same amount of cement clinker [4]. Moreover, lower calcination temperature is required for MK production than that needed to produce cement clinker. About 2.2 MJ energy is consumed by producing one ton of MK, compared to 1/5 of the energy consumed by cement production [5].

MK has a higher pozzolanic reactivity than other SCMs, such as fly ash and ground granulated blast furnace slag [6,7]. MK can react with

calcium hydroxide (CH), one of the hydration products of OPC to form additional calcium silicate hydrates (C–S–H) and calcium aluminate silicate hydrates (C-A-S-H). Therefore, MK can enhance the strength and durability of cement-based materials [8–10]. However, the incorporation of MK in cementitious systems can significantly reduce the workability of blended cement mixtures. Chemical admixtures such as water-reducers are usually needed to produce the required workability for the concrete [11,12].

Existing water reducers are mainly produced from petrochemical products [13,14] or derived from some renewable resources [15]. Aiming to broaden the range of molecules and polymers for interaction with cement, this study explores another renewable alternative admixture for MK blended cement. This admixture is L-ascorbic acid (AA), also known as vitamin C, which is a naturally occurring compound that is water-soluble with a five-membered lactone ring and four hydroxyl groups, as shown in Fig. 1. Our previous work [16] has demonstrated that AA can perform as a set retarder for calcium sulfoaluminate cement (CSA) by adsorbing on CSA grains and forming a complex with Ca²⁺. Similarly, AA can be adsorbed on the surface of OPC particles through

E-mail address: jwang@eng.ua.edu (J. Wang).

^{*} Corresponding author.

Fig. 1. Structural formula of AA.

electrostatic interaction between the acidic group and positively charged calcium ions on the surface of clinker and MK. This generates a electrostatic dispersing force between cement particles, allowing AA to be used as a water reducer for MK blended cementitious materials. Notably, this new admixture overcomes the major challenge of MK blended cement and significantly improves the performance of mortar and concrete made with this cement, resulting in higher eco-efficiency of the cement. In this way, AA can be used as a water reducer for MK blended cementitious materials.

Compared to existing fossil fuel-based chemical admixtures, biomass-derived products like AA have obvious advantages in terms of sustainability since they are renewable and nontoxic. AA is naturally occurring and can be found in various plants, including fruits and green vegetables [17,18]. AA is primarily produced by the breakdown of corn starch with heat and enzymes, acetone and HCl [19]. AA also can be abstracted from natural plants [20] and microorganisms [21]. More importantly. AA possesses multiple functions, such as water reduction. strength enhancement, and shrinkage reduction. More importantly, AA can inhibit the corrosion of steel enforcement [22,23]. Fuchs-Godec et al. demonstrated that 10^{-2} and 10^{-3} M of AA exhibited favorable inhibition efficiency for SS-type X4Cr13 steel in HCl solution [24]. This is attributed to the chemical reactivity of the hydroxyl groups on the enol-form ring of AA, which provide sites for the complexation or cross-linking of macromolecules or metal ions [25,26]. Xu et al. [27] investigated the effect of vitamin B3, B6 and C as a corrosion inhibitor on the ordinary Portland cement hydration. The results showed that AA has the most significant influence on compressive strength of concrete. When 0.40 % AA is added, the hydration reaction was almost stopped. Argiz et al. [28] used the AA as a green steel corrosion inhibitor to reduce chloride-induced corrosion in mortar. The highest efficiency of AA as a corrosion inhibitor can be reached with the addition of a concentration of 10⁻³ mol/L in the mixing water. Compared with other water reducing compounds, AA also has some drawbacks. Firstly, the price of AA is may higher than that of some water reducing agents. Secondly, the addition of AA delays the hydration of cement and reduces early-age strength of cementitious materials.

2. Raw materials and test methods

2.1. Raw materials

The OPC and MK were used as the main binder for all mortar and paste specimens prepared in this study. The median diameters (D50) of the OPC and the MK are 20 μm and 4.1 μm , respectively. Their oxide compositions based on X-ray fluorescence (XRF) analysis are shown in Table 1. The mineral contents of C3S, C2S, C3A and C4AF in the OPC

calculated by Bogues equation were 53.08 %, 25.74 %, 8.61 % and 7.82 %, respectively. River sand with 0.95 % water absorption was used as the fine aggregate and was purchased from a local distributor. The AA was added into the paste/mortar samples through dissolving in the mixing water (deionized water) before the mixing.

2.2. Preparation and characterization of mortar specimens

In this study, all mortar specimens were prepared using a constant water to binder ratio (W/B) of 0.50. The mix proportions of the specimens are listed in Table 2. The "Control" group was used as a reference and was prepared without the addition of MK and AA. The MK blended cement mortar groups were prepared by replacing OPC with 5 %, 10 %, and 20 % MK by mass, labeled as 5%MK, 10%MK, and 20%MK, respectively. Four different rates of AA (0.05 %, 0.1 %, 0.2 %, and 0.4 % by weight of total binder, OPC + MK) were added to the mortars. To better understanding the behavior of AA, cement mortars were also made with a commonly used retarder, sodium gluconate (SG) as a reference admixture added at 0.1 % and 0.2 % by weight of total binder. The mixing process involved adding the fine aggregates, cement, and MK, followed by the addition of the prepared AA solution into the dry mixture. The mixing bowl was made with stainless steel. Its capacity is approximately 4.73 L with 202 mm diameter and 175 mm depth. Before mixing, the inner wall of the mixing bowl was wetted with a damp towel. To make mortar without MK, the fine aggregates, and cement were put into the mixing bowl and mixed for 120s at speed of 140r/min \pm 5r/min before the prepared AA solution was pure into the dry mixture. The mixture was then mixed for 60s at speed of 140r/min \pm 5r/min. Then the mixer was stopped so that paste spread on sides of the mixing bowl can be scraped down into the batch. After that, the mixture was further mixed at speed of 285r/min±10r/min for another 60s. The MK blended mortars were prepared in the similar way. The major difference is that the MK was first added into AA or SG solution and stirred for 5 min. The

Table 2 Mix proportions of mortars (kg/m³).

Groups	Water	Cement	River sand	MK	AA
Control	269	535	1396	0	0
0.05%AA	269	535	1396	0	0.2675
0.1%AA	269	535	1396	0	0.535
0.2%AA	269	535	1396	0	1.07
0.4%AA	269	535	1396	0	2.14
0.1%SG	269	535	1396	0	0.535
0.2%SG	269	535	1396	0	1.07
5%MK	269	508.25	1369	26.75	0
10%MK	269	481.5	1369	53.5	0
20%MK	269	428	1369	107	0
5%MK0.05%AA	269	508.25	1396	26.75	0.2675
5%MK0.1%AA	269	508.25	1396	26.75	0.535
5%MK0.2%AA	269	508.25	1396	26.75	1.07
5%MK0.4%AA	269	508.25	1396	26.75	2.14
10%MK0.05%AA	269	481.5	1396	53.5	0.2675
10%MK0.1%AA	269	481.5	1396	53.5	0.535
10%MK0.2%AA	269	481.5	1396	53.5	1.07
10%MK0.1%SG	269	481.5	1396	53.5	0.535
10%MK0.2%SG	269	481.5	1396	53.5	1.07
10%MK0.4%AA	269	481.5	1396	53.5	2.14
20%MK0.05%AA	269	428	1396	107	0.2675
20%MK0.1%AA	269	428	1396	107	0.535
20%MK0.2%AA	269	428	1396	107	1.07
20%MK0.4%AA	269	428	1396	107	2.14

Table 1
Chemical compositions (%) of OPC and MK.

Oxide Composition	CaO	SiO_2	Al_2O_3	MgO	Fe ₂ O ₃	K ₂ O	TiO ₂	Na ₂ O	SO_3	LOI
OPC	64.85	22.94	4.89	3.52	2.57	0.81	0.21	0.20	1.81	2.52
MK	0.13	59.41	30.83	2.21	1.42	1.34	0.51	2.71	0.04	0.68

resulting MK slurry was then added into the dry mix of fine aggregate and cement, which was mixed for 120s at speed of 140r/min \pm 5r/min in the mixing bowl. Resulting fresh mortar was poured into molds to create 50.8 mm \times 101.2 mm (2 in. \times 4 in.) cylinders. The mortar specimens were sealed in molds for 24 h at 23 °C \pm 1 °C. Then they were demolded and cured in a curing room with temperature at 23 °C \pm 1 °C and relative humidity (RH) above 95 % until the tests were conducted. Compressive strength tests were performed at 3d, 7d, 28d, and 90d, and the average value of three replicated mortar specimens was calculated and measured as the compressive strength. The Mercury intrusion porosimetry (MIP) test was used to analyze the porosity and small capillary pores of the mortar samples at 28d.

2.3. Flowability

Flow table test was conducted to characterize the flowability of fresh mortars for all groups according to ASTM C1437 [29]. The diameters of two orthogonal directions of mortar spread were measured and the average diameter of the orthogonal directions was reported as the flowability of fresh mortar.

2.4. Isothermal calorimetry test

Isothermal calorimetry test was conducted according to ASTM C1702 [30] to evaluate the effect of AA on the hydration of cementitious material with a water to binder ratio (W/B) of 0.5. An I-Cal 2000HPC calorimeter was used to measure the heat flow and cumulative hydration heat of the pastes. To produce the paste for the "Control" group, 25 g deionized water was added to 50 g cement and mixed for 120 s at a baseline temperature of 23 °C. The resulting fresh paste was then immediately placed in the calorimeter. The pastes with MK and AA or SG were produced in a similar way. First, 50 g of cementitious materials (cement and MK) were mixed in a mixer for 60 s, followed by the addition of 25 g of prepared AA or SG solution. After 120 s of mixing, the fresh paste was then placed in the calorimeter immediately. The heat release from hydration was measured for the first 72 h.

2.5. Characterization of hydration products

The cement pastes after isothermal calorimetry test were used for X-ray diffraction (XRD) and thermogravimetric analysis (TGA). The XRD patterns of the paste samples were obtained by scanning from 10° to 60° with rate of 5° 20/min by Cu Ka radiation at 45 kV and 200 mA. TGA was carried out to evaluate contents of the hydration products. The sample was placed in a chamber for heating with a heating rate of 10 °C per minute from 30 °C to 800 °C. The content of bound water (BW) can be calculated by the percent of mass loss from 40 °C to 550 °C base on the thermogravimetric (DTG) curves [31] as

$$W_{BW} = (M_{40} - M_{550}) / M_{550} \times 100\%, \tag{1}$$

where W_{BW} is the content of hydrated water (HW), M_{40} is the weight of sample at 40 °C, and M_{550} is the weight of sample at 550 °C.

The decomposed calcium hydroxide (CH) was calculated by integrating the DTG curve from 400 $^{\circ}$ C to 500 $^{\circ}$ C [32]. The content of CH was normalized by the dry binder mass at temperature of 550 $^{\circ}$ C [31] as

$$W_{CH} = \frac{M_{400} - M_{550}}{M_{550}} \times \frac{74}{18} \times 100\%, \tag{2}$$

where W_{CH} is the content of HW, M_{400} is the weight of sample at 400 °C, M_{500} is the weight of sample at 500 °C, and 74 and 18 are molecular masses of CH and water, respectively.

2.6. Nanoindentation test

The nanoindentation test was implemented to characterize nano-

mechanical property of hardened cement pastes by a Hysitron TI-950 triboindentor. The tests were conducted using a load control method, with a maximum load of 1 mN. To minimize the effect of creep [33], the maximum load was reached through nine loading steps, as depicted in Fig. 2. At the end of each step, the maximum load was maintained for 2 s, and then the load was gradually reduced to zero over a period of 5 s. During the final unloading step, the load and displacement were automatically recorded for analysis. The nanoindentation modulus was calculated by [34].

$$M = \frac{\sqrt{\pi}}{2\beta} \bullet \frac{S}{\sqrt{A_c}},\tag{3}$$

where, M is the indentation modulus, S is the contact stiffness, β is the calibration coefficient of. the indenter, and A_c is the contact area at the maximum load. The elastic modulus was calculated by

$$\frac{1}{M} = \frac{1 - \nu^2}{E} + \frac{1 - \nu_i^2}{E_i},\tag{4}$$

where, E and ν are elastic modulus and Poisson ratio of the mortar sample, respectively; E_i and ν_i are elastic modulus and Poisson ratio of the indenter, respectively.

After the elastic modulus of each point was calculated, the deconvolution process was implemented based on Gauss Mixture Model using MATLAB. The phases of calcium silicate hydrate (C–S–H) were identified by the values of elastic modulus in indent area. The C–S–H packing density was calculated by the following formula:

$$\eta_i = 0.5(M_i / m_s + 1),$$
 (5)

where, η_i is packing density of indent area, M_i is indentation modulus of each indentation test point, m_s is indentation modulus of solid phase, which is 62.5 GPa for solid C–S–H according to the existing report [35].

2.7. Autogenous shrinkage

The autogenous shrinkage test was conducted to evaluate volume stability of cement pastes at early age using corrugated pipes with a length of 420 mm and an outer diameter of 29 mm according to ASTM C1698 [36]. The fresh cement paste was cast in the corrugated plastic pipe mold, and then placed in a thermostatic curing room at 23 °C \pm 1 °C. After the final set of the cement paste, the length of specimen was measured as the initial length (L_0). The autogenous shrinkage (μ_{as}) was calculated by

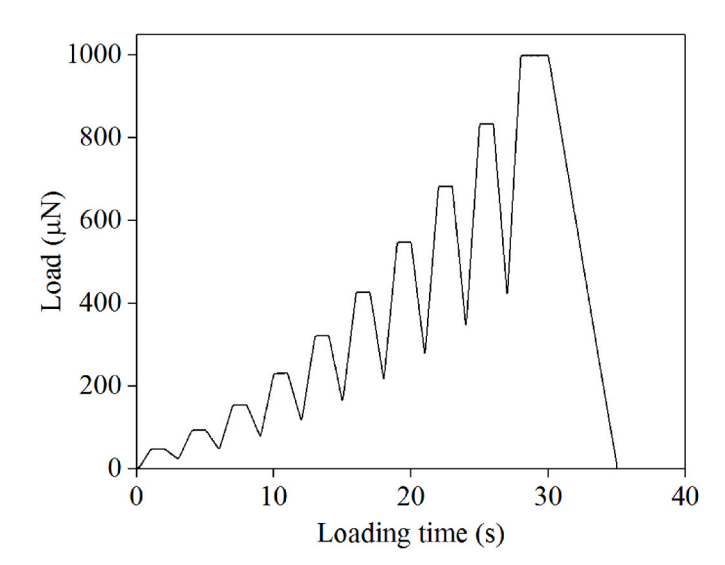


Fig. 2. Load function of nanoindentation.

$$\mu_{as} = \frac{L_i - L_0}{L_0},\tag{6}$$

where L_i is the length of the specimen.

2.8. Reinforcing bar corrosion

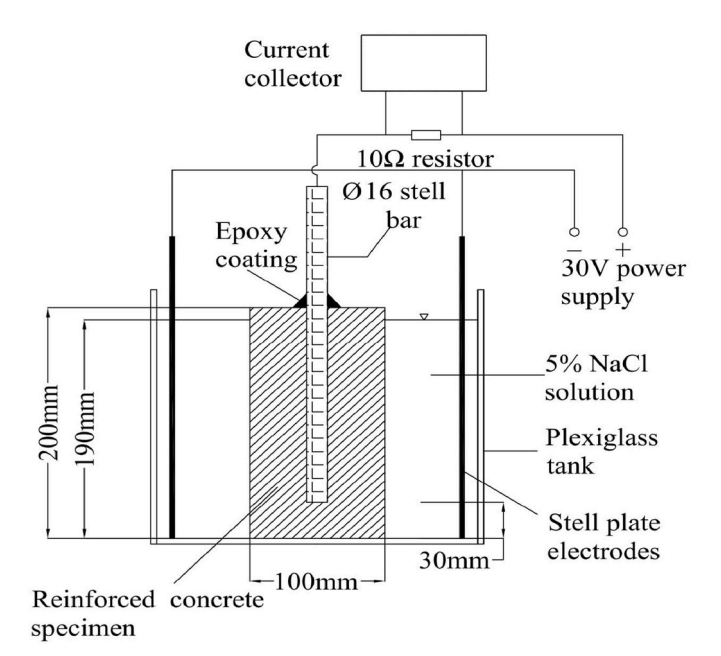
A rapid corrosion test was performed using an electrochemical corrosion method to assess the ability of AA to inhibit the corrosion of a reinforcing bar (rebar) embedded in mortar [37]. The testing system used is illustrated in Fig. 3. The fresh mortar was prepared with the same mix proportions as presented in Table 2, and then cast into cylinder molds with dimensions of 100 mm diameter and 200 mm height. To remove bubbles inside the mortar, the mold was placed on a vibration table for 30 s. Next, a 16 mm diameter steel rebar was embedded in the mortar. After 48 h of curing in a room with a temperature of 23 °C \pm 1 °C and relative humidity (RH) of at least 95 %, the specimen was immersed in a 5 % NaCl solution, as shown in Fig. 3. The rebar was connected to the positive pole, while two aluminum plates were connected to the negative electrode in the solution. When the 30 V constant voltage power supply was turned on, the electric current was automatically recorded by the current collector. The current will suddenly increase when a crack is formed from the rebar to the side surface of the specimen. The corresponding time was recorded as the corrosion time to evaluate the corrosion resistance of the specimen.

3. Results and discussions

The "Control" in figures and tables refer to the mortar or paste prepared without AA and MK. "0.05%AA", "0.1%AA", "0.2%AA" and "0.4%AA" refer to the percentages of AA by weight of cementitious materials. Similarly, "0.1%SG" and "0.2%SG" refer to the percentages of SG by weight of cementitious materials. "5%MK", "10%MK" and "20% MK" refer to the MK replacement levels.

3.1. Water-reducing capability of AA

The impact of AA on the flowability of fresh mortar is shown in Fig. 4. As expected, the higher surface area of MK leads to a reduction in the flowability of fresh mortars. To counteract this, water reducers are commonly employed to achieve the desired workability for concretes



 $\textbf{Fig. 3.} \ \ \textbf{Electrochemical corrosion test system [37]}.$

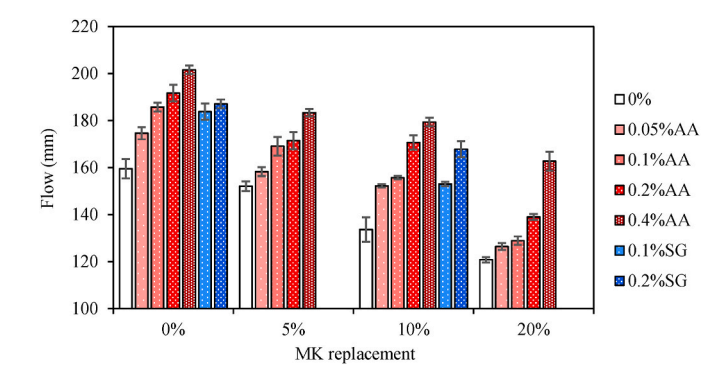


Fig. 4. Flowability test results of mortar and MK blended mortar made with and without AA.

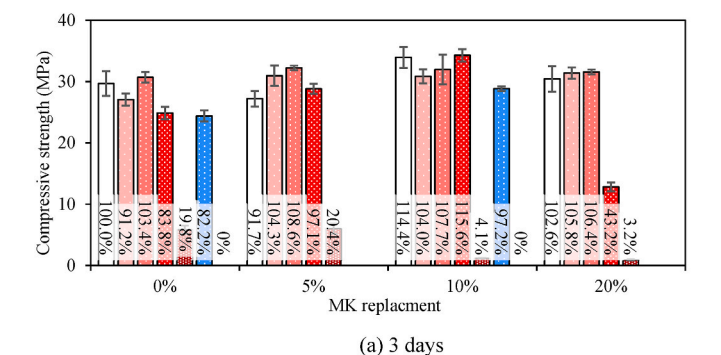
with MK. However, the addition of AA can alleviate this decrease in workability induced by the inclusion of MK. Fig. 4 indicates that the flowability increases with the quantity of AA added, validating its function as a water reducer. Compared with the AA, flowability of fresh mortar with SG is slightly lower, as shown in Fig. 4. AA comprises four hydroxyl groups, one of which dissociates in aqueous solutions. The acidic group interacts with positively charged calcium ions on the surface of cement particles, enabling AA to be adsorbed on their surface. Additionally, the remaining hydroxyl groups help to disperse the particles in aqueous systems [38]. Consequently, the workability of mortar is improved with the addition of AA. Moreover, the OPC/MK mixes have lower flowability than mixes only with OPC, which is requiring high dosages of AA to restore flowability.

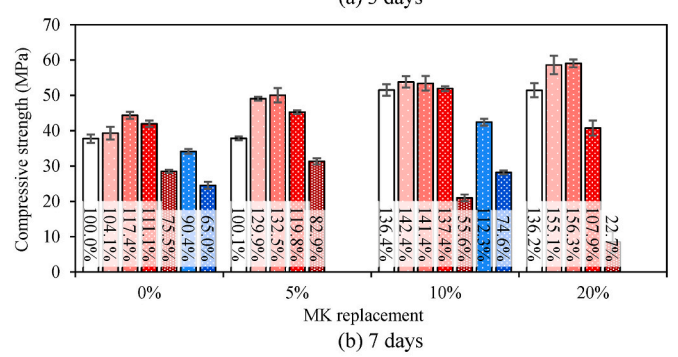
3.2. Compressive strength of mortar

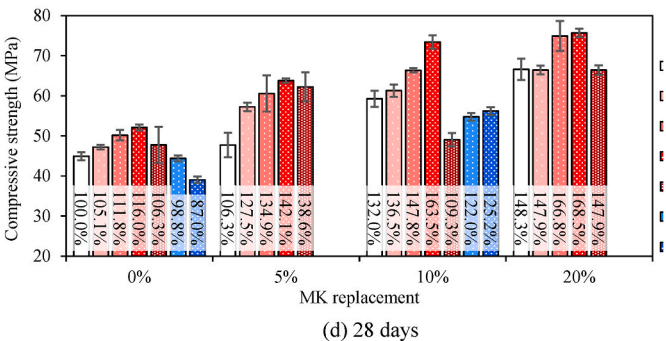
Fig. 5 illustrates the compressive strengths of various mortars at 3d, 7d, 28d, and 90d. The percentage values in each column represent the ratio of the compressive strength to the corresponding value of the control group. At 3d, the compressive strength of the mortar containing 5 % MK is slightly lower than that of the control group. This is because the pozzolanic reaction between MK and CH is slower than the hydration of OPC. However, at higher substitution levels (10 % and 20 %), the compressive strengths of cement mortars with MK exceed that of the control group. This is due to the high specific surface area of MK powders, which seed cement hydration at an early age, resulting in an accelerating effect. After 3d, the compressive strengths of all mortars with MK surpass that of the control sample, indicating the high pozzolanic activity of MK or densification of the cementitious paste. Thus, the compressive strength of mortar can be increased by increasing the content of MK, owing to its high pozzolanic reactivity. By substituting 20 % of OPC with MK, the compressive strengths at 28d and 90d are enhanced by over 48 % and 44 %, respectively, as presented in Fig. 5(c) and (d).

The lower compressive strength of the mortar with AA at 3d indicates that AA can significantly retard cement hydration. At this age, the compressive strength of the mortar with 0.4 % AA is 80 % lower than that of the one without AA. However, the effect of retardation diminishes at 7d. Except for the sample with 0.4 % AA, all mortar samples with AA are stronger than the control group at this age. Afterward, the compressive strengths of all mortar specimens with AA surpass that of the control group. Notably, the compressive strength of the mortar at 90d increases with the content of AA, and an increment of 27.8 % in compressive strength is achieved by adding 0.4 % AA. Clearly, AA can contribute to a significant increase in late age compressive strength.

Fig. 5 illustrates that the effects of AA on the compressive strengths of MK blended cement mortars are similar to those observed in the cement-only mortar. Firstly, the addition of AA significantly retards the early age strength development of these mortars. At 3d and 7d, the compressive







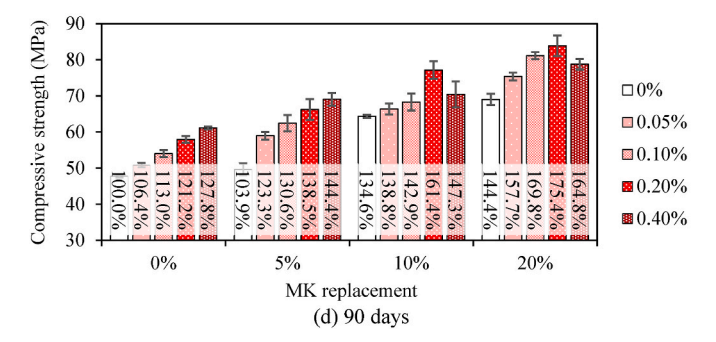


Fig. 5. Compressive strengths of the cement mortars and MK blended mortars at different ages: (a) 3d; (b) 7d; (c) 28d; (d) 90d.

strengths of the MK blended cement mortars decrease dramatically with the addition of more than 0.2 % AA. The relative content of AA by mass of cement is higher in these OPC/MK blended mortars due to less OPC and the same amount of AA present, leading to a stronger retarding effect. Secondly, the addition of AA can significantly enhance the compressive strength of the MK blended cement mortars. For example, the addition of 0.05 %, 0.1 %, 0.2 %, and 0.4 % AA to mortar with 5 % MK increases its compressive strength at 28d by 27.5 %, 34.9 %, 42.1 %, and 38.6 %, respectively. However, the compressive strength of mortar with 0.4 % AA is slightly lower than that of the mortar with 0.2 % due to the stronger retarding effect. The same trend can be seen from the compressive strengths of cement mortars with 10 % and 20 % MK at this

age, as shown in Fig. 5(d). At 90d, the compressive strength of mortar with 5 % MK increases with the content of AA, indicating that the retarding effect of 0.4 % AA on the mortar is fully recovered. This demonstrates the potential of AA as a late strength enhancer for MK blended cement mortar. The addition of 0.4 % AA increases the compressive strength by 44.4 % for this mortar, which is much higher than the 3.9 % achieved by only replacing 5 % OPC with MK without any AA. Similar strength improvements have been achieved by adding AA to mortars with 10 % and 20 % MK, as shown in Fig. 5(c) and (d). Once again, late age compressive strength of the MK blended cement mortar can be significantly increased by AA.

Improving the compressive strength of mortar and concrete without using more cementitious materials is crucial for enhancing the material efficiency of cement. This is because it allows for achieving a desired strength with less cement or reducing the amount of concrete needed during construction due to the higher strength. As a result, this approach can significantly reduce carbon emissions, benefiting the environment at the expense of slightly lower early age strength.

As comparison, effects of SG on the strength of the cement mortars are also presented in Fig. 5. At the same dosage, the compressive strengths of the cement mortars with SG are much lower than that with AA at all tested ages (3d, 7d and 28d). At the same dosage, the compressive strength of the mortars with SG are lower than that of the one with AA for all testing ages (3d, 7d and 28d), confirming the advantage of AA to enhance the strength of concrete. Addition of 0.1 % SG reduces the compressive strength of the mortar at 3d by 17.8 % in comparison with the control one. This reduction decreases at 7d and 28d because the retarding effect of the SG diminishes as age increases. When 0.2 % SG is added, the mortar has no strength at 3d because of the strong retarding effect of SG. Although the compressive strength of this mortar increases rapidly after 3d, it is still lower than that of the control group. Similar trend of the compressive strength growth is observed for the MK blended mortar with SG. The compressive strength increases slowly in the early stage and rapidly in the later age. Once again, the compressive strength of mortar is reduced by the addition of SG in comparison with the MK blended mortar without the additive.

3.3. Hydration heat evolution

The results of the calorimetry test on cement pastes with AA are presented in Fig. 6. It can be observed from Fig. 6(a) that the hydration of cement is delayed by the presence of AA, resulting in longer induction periods and lower exothermic peaks. This is not surprising since AA tends to get adsorbed on the surface of cement particles, thus hindering the dissolution process of cement particles. One of the main reasons for set retardation is a delay in calcium hydroxide precipitation due to complexing of calcium with AA. The degree of retarding effect increases with the increase in the amount of AA added to the paste, leading to lower compressive strength of mortar with a high dosage of AA at an early age, as depicted in Fig. 5. Fig. 6(b) shows a comparison of the accumulated hydration heat of the cement paste samples with and without AA. It is evident that the accumulated hydration heat is significantly reduced in the presence of AA. Interestingly, the cement pastes with AA exhibit a higher accumulated hydration heat in the first 3 h than the control paste, indicating the occurrence of an exothermic reaction between AA and alkali in the cement paste. Assuming the SO₃ of MK is low, the SO₃ content can decreases in the cementitious system, which would potentially cause an increase in C₃A hydrate. Therefore, it is possible that AA affects the balance of aluminate reactivity and sulfate availability, leading to the formation of a small amount of C₃A hydrate. The main reason for delayed setting of cement is the hydroxyl group in AA. When AA is added, hydroxyl group may adsorb on the surface of cement particles, leading to inhibition of cement hydration reaction. This retarding effect makes the more uniform distribution of hydration products in the solution around cement particles. For this reason, the set retardation is a delay in calcium hydroxide precipitation due to

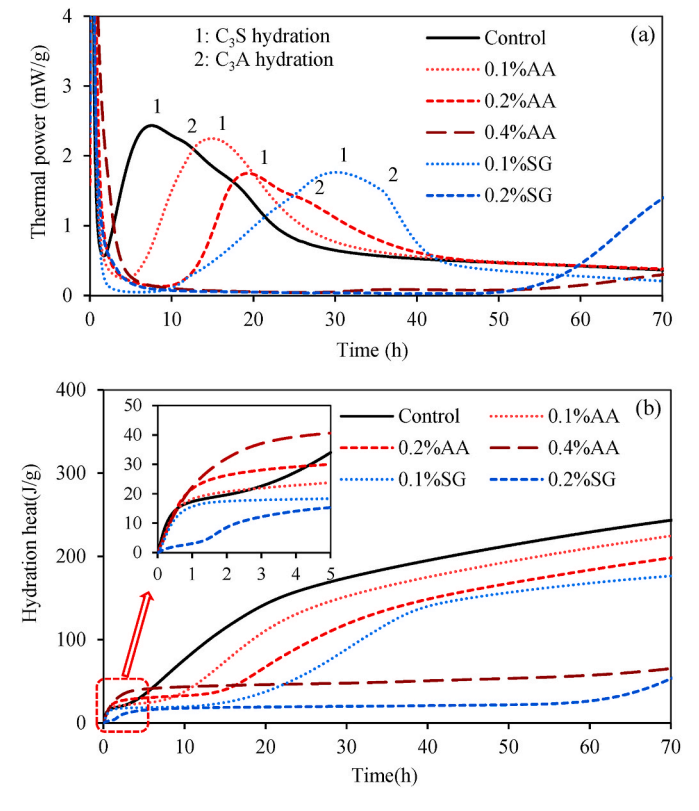


Fig. 6. Effect of AA on cement hydration: (a) thermal power; (b) hydration heat.

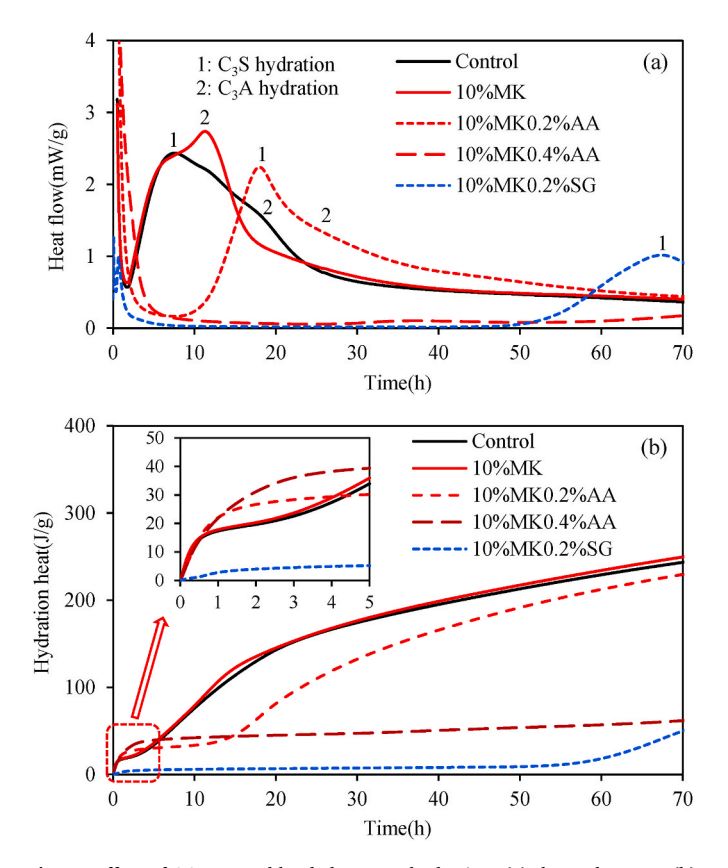


Fig. 7. Effect of AA on MK blended cement hydration: (a) thermal power; (b) hydration heat.

complexing of calcium with AA.

Fig. 7 presents the calorimetry test results of MK blended cement pastes prepared with AA. The results show that replacing 10 % of OPC with MK greatly enhances the hydration of the aluminate phases, as indicated by the higher aluminate peak corresponding to sulfate depletion of this paste. This increase in the aluminate peak can be attributed to the higher surface area of MK, which provides more nucleation area for cement hydration [39], and the aluminate content from MK that can introduce an under-sulfated condition during the initial hydration processes. Despite this, the accumulated hydration heats of the pastes with AA are still lower than that of the paste without AA at the end of the calorimetry testing (70 h). However, the high surface area of MK appears to mitigate some of the retarding effects of AA, and the accumulated hydration heat of the MK blended mortar sample with 0.1 % AA is closer to that of the control paste compared to the paste sample without MK (Fig. 5(b)). For the MK blended mortar, the MK was first mixed with AA solution. Some AA molecules can be absorbed on the MK due to the high specific surface area and good adsorption ability. During this process, the free AA molecules in the AA solution was decreased. The retarding effect can be weakened when AA is mixed with cement. Moreover, the secondary hydration reaction between MK and cement is slowed down due to the adsorption of these AA molecules on MK. For those reasons, mortar properties can be effective improvement at later ages.

In Figs. 6 and 7, the hydration of cement was strongly retarded as sodium gluconate was added. At the same dosage, SG has a more powerful and long-lasting retarding effect as shown in Fig. 6. Cement hydration was almost blocked at first 60 h when 0.2%SG was used. When the SG concentration decreases to 0.1 %, the peak of C3S hydration heat release is delayed to 30 h. This retarding effect leads to slow growth in compressive strength at first 3d. For MK blended mortar, SG also has more powerful and long-lasting retarding effect as shown in Fig. 7. Cement hydration is blocked at first 60 h, leading to no compressive strength at 3d and lower compressive strength at 7d and 28d compared with the same dosage of AA. SG has a stronger retarding effect compared to AA, leading to the reduction in compressive strength of mortar. The hydration of cement is more sensitive to the dosage of SG, so it is necessary to control the dosage of SG more accurately.

3.4. Hydration products of cement pastes

Fig. 8 presents the XRD patterns of hardened cement paste samples at different ages, including 3d, 7d, 28d, and 90d. The un-hydrated cement contains minerals such as C_2S , C_3S , and C_3A , which can be seen in Fig. 8. The major crystalline hydration products, including ettringite (AFt) and calcium hydroxide (CH), are clearly visible in the XRD spectra. It is worth noting that the presence of $CaCO_3$ in the cement paste samples is expected due to the common use of limestone as a filler in cement. Additionally, some of the hydration products such as CH can easily undergo carbonation, leading to the formation of $CaCO_3$. However, the XRD patterns do not show any clear peaks corresponding to calcium silicate hydrate (C–S–H) due to its poorly crystalline structure, which makes it difficult to detect using XRD.

The results in Fig. 8(a) and (b) indicate that the cement pastes with AA had a higher content of C_2S , C_3S , and C_3A at early ages (3d and 7d), suggesting a significant retardation of hydration by AA. This observation is consistent with the calorimetry results shown in Figs. 6 and 7. The lower amount of CH detected in the pastes with AA compared to those without AA also supports this conclusion. CH is produced during cement hydration, and a lower amount of CH in the pastes with AA indicates a lower degree of hydration compared to those without AA. Additionally, the presence of AFt in the pastes with AA suggests that AA retards the transformation of AFt to AFm.

At later ages (28d and 90d), the intensities of C_2S , C_3S , and C_3A in all samples are similar, indicating that the retarding effect of AA diminishes over time. AFt is undetectable in all pastes at these ages, suggesting that

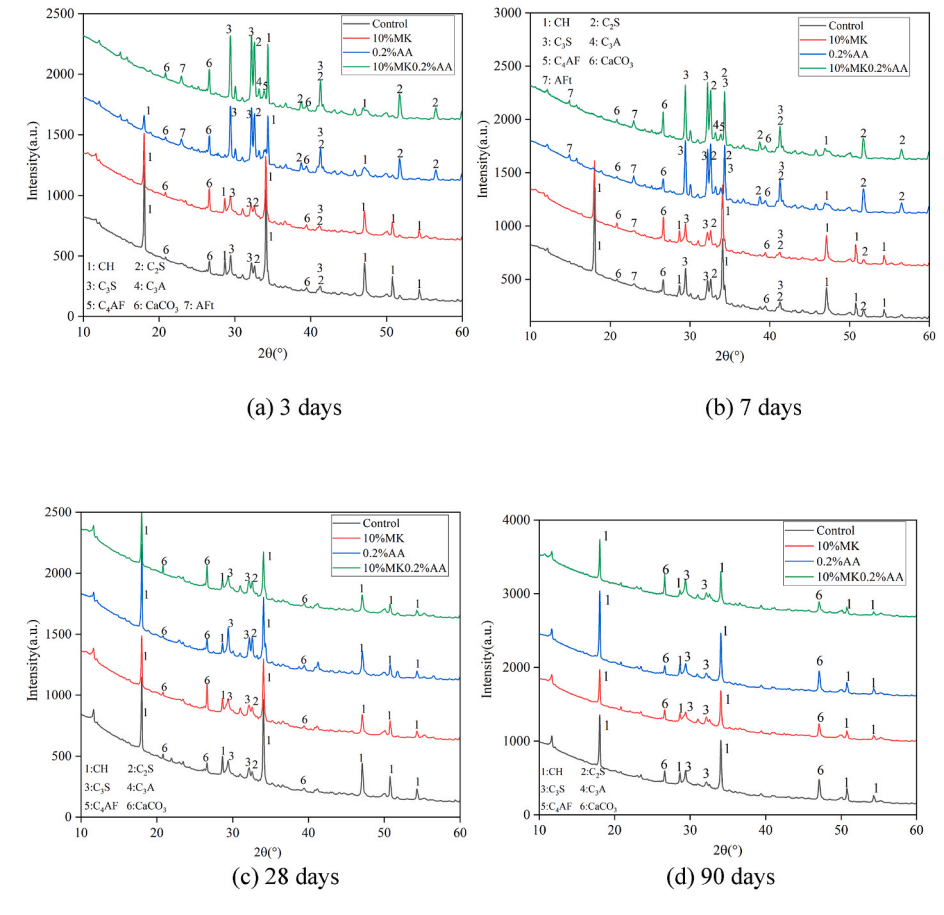


Fig. 8. XRD patterns of cement pastes and MK blended cement paste with and without AA at different ages.

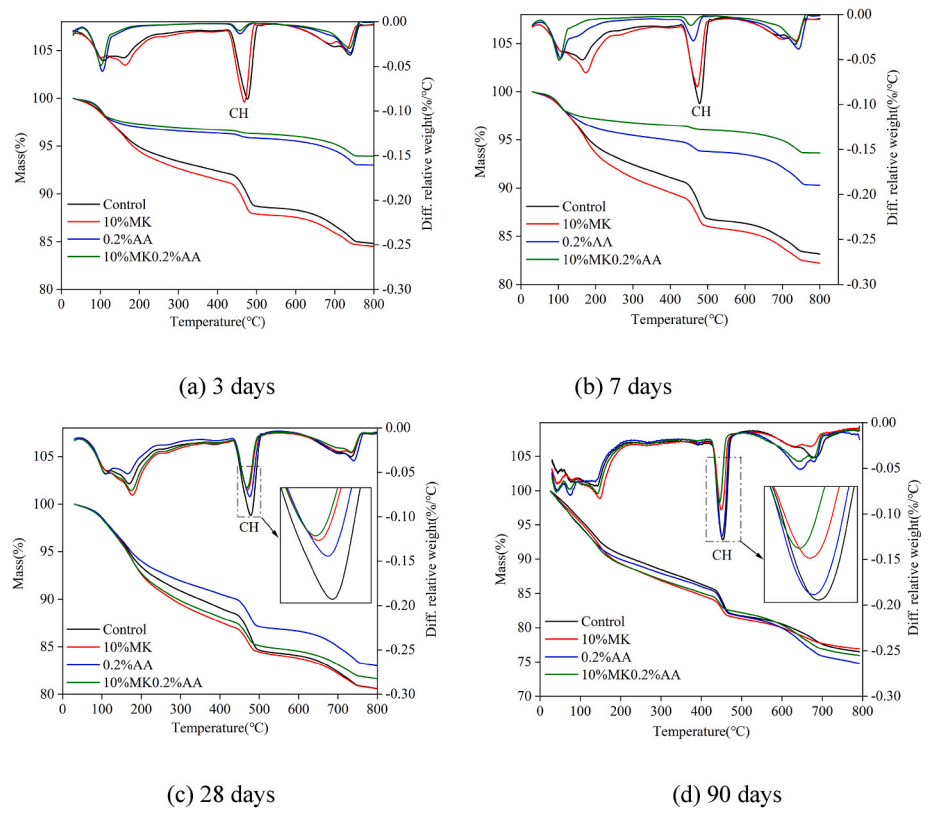


Fig. 9. TGA results of cement pastes and MK blended cement paste with and without AA at: (a) 3d; (b) 7d; (c) 28d; (d) 90d.

most of it has been transformed into AFm. Fig. 8(c) and (d) also show that the CH content in the samples with MK is lower than those without AA, indicating that a pozzolanic reaction occurred between MK and CH, consuming some CH. It is important to note that while XRD patterns can provide qualitative analysis of cement hydration products, TGA is necessary for quantitative analysis.

The TGA results of hardened cement paste samples at 3d, 7d, 28d, and 90d are shown in Fig. 9. These results were used to calculate the contents of BW and CH using Eqs. (1) and (2) and are presented in Table 3. As expected, the contents of CH and BW in the cement paste containing 0.2 % AA are lower than those in the control sample, confirming the retarding effect of AA on cement hydration. However, this difference decreases with age, suggesting that the retarding effect of AA decreases as the cement paste continues to hydrate. Upon the addition of MK, the pozzolanic reaction can consume some CH. Therefore, the CH contents in the two paste samples containing MK are much lower than that in the control sample. In contrast to the control sample, where the CH content increases with age, CH content of the sample with 10 % MK decreases with age because of the ongoing pozzolanic reaction between MK and CH.

Interestingly, the contents of CH in the two samples with AA are significantly reduced at early ages (3d and 7d). This reduction can be attributed not only to the retarding effect of AA but also to the reaction between AA and CH. Consequently, the hydration degree of each paste can only be evaluated by the BW content. Table 3 shows that the sample with 10 % MK has slightly more BW at all ages than the control sample. This suggests the cement hydration is slightly accelerated by replacing 10 % of the cement with MK. This observation is consistent with the calorimetry test results shown in Fig. 7(b). At a late age (90d), no significant difference is found in the contents of BW among all samples, indicating that a similar degree of hydration has been achieved by all samples. However, the 10 % MK 0.2 % AA paste has the lowest content of CH, even lower than the 10 % MK sample, confirming that some CH was reacted with AA.

3.5. Pore size distribution of mortar sample

Figs. 10 and 11 offer insights into how the substitution of OPC with MK affects the microstructure of hardened mortar. Fig. 10(a) shows that the addition of MK significantly decreases the total porosity of hardened mortar, which is attributed to the increased production of C–S–H resulting from the reaction between MK and CH. Additionally, since MK has a very small particle size (D50 $=4.1~\mu m$), it acts as a filler similar to silica fume and reduces the size of capillary pores, resulting in a denser microstructure of the mortar. This denser microstructure contributes to higher compressive strength of the mortar, as compared to the control

Table 3
Weight contents of bound water (BW) and calcium hydroxide (CH).

Groups	Ages (days)	BW (wt. %)	CH (wt. %)		
Control	3	11.37	12.13		
	7	13.31	13.20		
	28	15.56	13.61		
	90	18.02	13.44		
10%MK	3	12.11	11.55		
	7	14.15	9.83		
	28	15.78	7.69		
	90	18.34	7.32		
0.2%AA	3	4.18	1.36		
	7	6.21	3.04		
	28	13.01	9.95		
	90	17.97	11.22		
10%MK0.2%AA	3	3.67	0.86		
	7	3.96	1.07		
	28	15.06	7.44		
	90	17.42	5.63		

sample.

The addition of 0.2 % AA to the 10%MK mortar leads to a further reduction in porosity, as shown in Fig. 10(a). This can be attributed to the plasticizing effect of AA, as indicated by Fig. 4. In addition, Fig. 10 (b) indicates that AA, through its retarding effect, significantly reduces the number of capillary pores below 50 nm. This suggests that the nanoscale structure of cement hydration products can be densified through the retarding effect of AA, which is a crucial factor responsible for the higher compressive strength of the 10%MK0.2%AA mortar, as shown in Fig. 5. The slower and more ordered build-up of hydration products induced by the significant retarding effect of AA is also likely responsible for the higher late-age compressive strength and lower pore volume of the mortar. Similar effects on the pore structure of the produced mortar have been observed with other biomolecules, such as tannic acid [40], possibly due to the high density of functional groups of these biomolecules that can interact with the hydration products. Interestingly, the critical size of the pore is enlarged by the addition of AA, as the denser hydration products occupy a smaller amount of space, as shown in Fig. 10(b).

In Fig. 11, the pore volume of capillary pores in four size ranges is shown: very harmful (>200 nm), harmful (100-200 nm), almost harmless (20–100 nm), and harmless (<20 nm) [41], as determined by MIP analysis. The addition of 10 % MK to the mortar resulted in a lower volume of harmful and very harmful capillary pores compared to the control sample, leading to a 32.0 % increase in compressive strength at 28 days (as shown in Fig. 5(d)). Moreover, the addition of retarding effect of the 0.2 % AA further reduced the volumes of harmful and very harmful pores, as depicted in Fig. 11. As a result, the compressive strength of the mortar improved by 63.5 % compared to the control sample. Although harmless and almost harmless pores have little impact on the compressive strength of the mortar, they play a crucial role in the shrinkage and creep of concretes. Fig. 11 shows that the sample with 0.2 % AA had the lowest volume of harmless and almost harmless pores, which indicates that the addition of AA can reduce the shrinkage of the produced cement mortar.

3.6. Nanoindentation analysis

Fig. 12 shows the elastic modulus mapping obtained by nano-indenation for 10%MK and 10%MK0.2%AA mortars at 90d. The areas of elastic modulus greater than 60 GPa correspond to the filler or unhydrated cement, while the areas with elastic modulus less than 60 GPa represent the hydration products of the cement. Fig. 12 clearly indicates that the sample with AA has more hydration phases with higher elastic modulus compared to the 10%MK sample. The average elastic moduli of all hydration phases in 10%MK and 10%MK0.2%AA samples are 19.57 GPa and 22.49 GPa, respectively. The addition of AA improves the average elastic modulus of the sample by more than 14.9 %, which is the main reason for the enhanced compressive strength of the mortar sample.

As shown in 12, the fitting curves for the porous phase (PP), low density (LD) C-S-H, high density (HD) C-S-H, and ultra-high density (UHD) C-S-H are shown by green, blue, black, and purple lines in, respectively; π , μ and σ represent the volume fraction of the phase, mean value of the modulus (in GPa), and its standard deviation (in GPa), respectively. The comparison between 10%MK and 10%MK0.2%AA samples reveals that the addition of AA reduces the volume fraction of LD C-S-H by 7 %, but increases the volume fraction of HD C-S-H by 11 %, consistent with the pore structures depicted in Fig. 11. The addition of AA considerably reduces the number of harmless pores, including gel pores, indicating an improvement for the density of the produced C-S-H. The 10%MK sample contains a significant amount (6 %) of UHD C-S-H, which is reduced to only 1 % by adding AA. Therefore, the addition of AA improves the homogeneity of the produced cement mortar. Meanwhile, the mean elastic modulus of all phases of the sample with AA are also higher than their counterparts without AA. All these

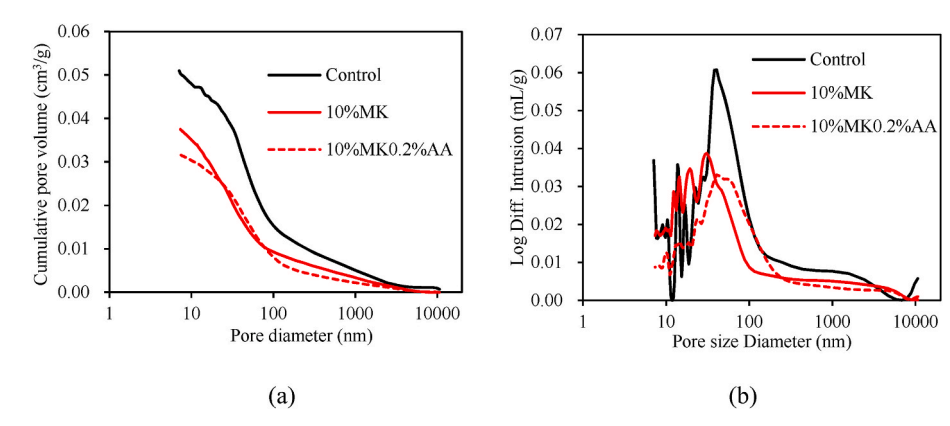


Fig. 10. Pore structure of the mortars with and without AA at 28d: (a) cumulative pore volume; (b) pore size distribution.

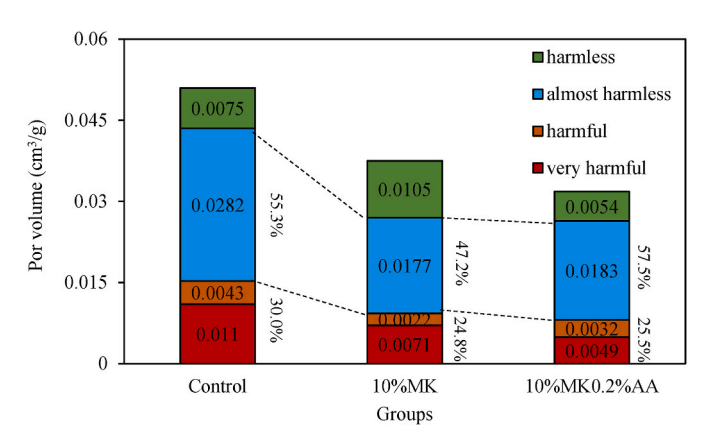


Fig. 11. Pore volume distribution verse sizes at 28d

contribute to improving the compressive strength of 10MKO.2%AA mortar. This can be seen more clearly from the packing densities of the hydration phases shown in Table 4, which shows that adding AA increases the packing density of hydrated products (C–S–H phases) by 0.021.

3.7. Autogenous shrinkage

The autogenous shrinkage behavior of four cement pastes from final setting to three weeks is illustrated in Fig. 13. The graph shows that the autogenous shrinkage of all samples slows down after 7 days, indicating that most of the autogenous shrinkage occurs within 7 days. When 10 % of the cement is replaced with MK, the autogenous shrinkage of the sample nearly doubles compared to the control sample at 7 days. This increase is due to the combined effect of accelerated cement hydration, pozzolanic reaction, and finer pore structure of the MK blended mortar. As depicted in Fig. 7, replacing 10 % of the cement with MK slightly accelerates the cement hydration process, leading to more self-desiccation of the mortar sample. Additionally, Figs. 10 and 11 show

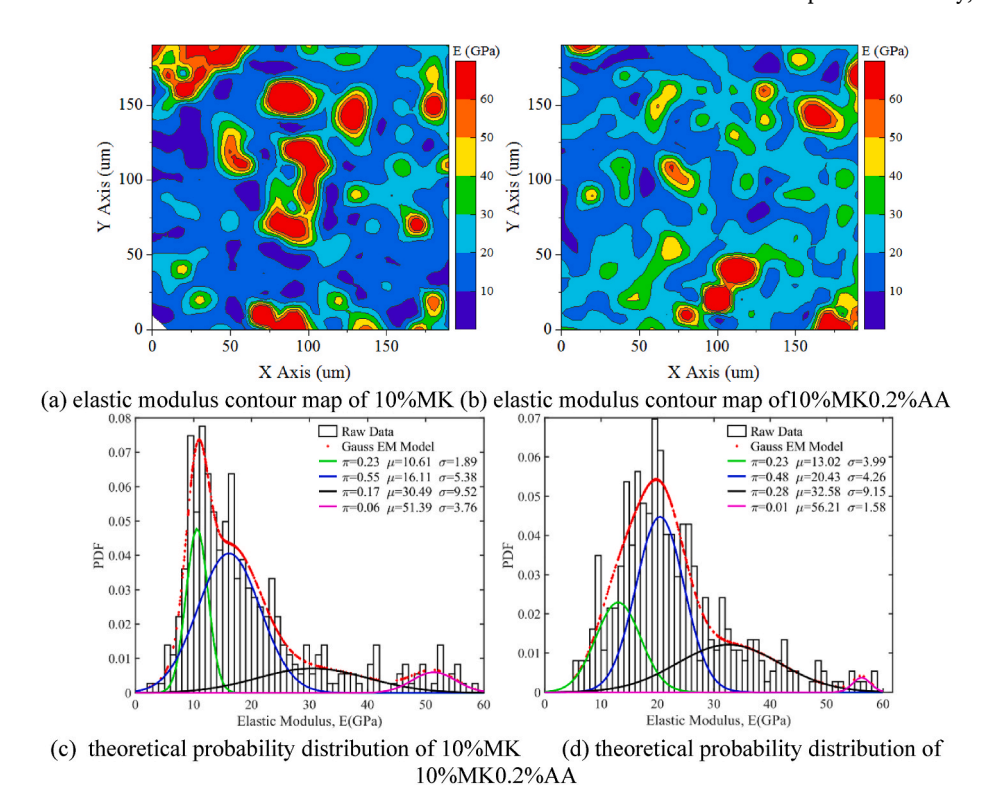


Fig. 12. Contour map of elastic modulus for indent area and theoretical probability distribution functions for elastic modulus data.

Table 4Packing density of different C–S–H phases from the nanoindentation results.

Groups	PP		LD		HD	HD		CH	
	Volume	Mean	Volume	Mean	Volume	Mean	Volume	Mean	
10%MK	0.23	0.59	0.55	0.63	0.17	0.75	0.06	0.93	0.666
10%MK0.2%AA	0.23	0.61	0.48	0.67	0.28	0.77	0.01	0.97	0.687

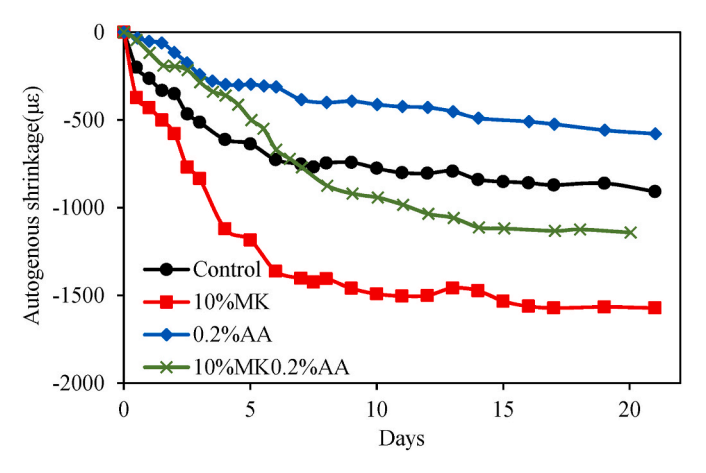


Fig. 13. Autogenous shrinkage of cement paste and MK blended cement pastes with and without AA.

that the addition of MK significantly reduces the pore sizes, generating more pores with sizes smaller than 50 nm. A prior study has suggested that capillary pores with sizes ranging between 5 nm and 50 nm mainly control the autogenous shrinkage [42]. Therefore, increasing capillary pores in this range can enhance the autogenous shrinkage. Such high autogenous shrinkage increases the risk of cracking in the early stages of the cement's life.

AA as an autogenous shrinkage reducer for cement mortar is clearly confirmed by Fig. 13. The excessive autogenous shrinkage observed in the 10%MK sample can be significantly reduced by adding 0.2 % AA. The autogenous shrinkage in the 10%MK0.2%AA sample is reduced by over 27 % compared to the 10%MK sample, as shown in Fig. 13. Figs. 10 and 11 reveal that the addition of AA can significantly decrease the capillary pores with size below 50 nm in the mortar, resulting in much lower autogenous shrinkage in the produced sample. Fig. 13 indicates that AA can reduce the autogenous shrinkage of cementitious material, which can be attributed to two main factors: lower degree of hydration at the early age and lower porosity induced by AA. As shown in Fig. 6 and 7, the hydration of the cement was significantly retarded by adding AA, which is beneficial for reducing the autogenous shrinkage of cementitious material at the early age. Fig. 10 reveals that the pore volume of the cementitious material was reduced by AA, further resulting in a decrease in autogenous shrinkage.

3.8. Reinforcement electrochemical corrosion

Concrete microcracks can allow harmful substances, such as chloride ions, water, and carbon dioxide, to infiltrate, which can lead to the electrochemical corrosion of reinforcing bars [43]. In Fig. 14, electrochemical corrosion current curves of rebars in mortar specimens are shown. Once corrosion begins, rust produced on the rebar's surface generates volume expansion, which can cause cracks. When cracks occur due to this expansion, the electrical resistance between the positive and negative poles is significantly reduced, leading to a sudden rise in current. The corrosion time of the sample is recorded as the time corresponding to this sudden increase in current. As shown in Fig. 14, the two samples with MK exhibit a much lower initial corrosion current due to their considerably lower permeability, as indicated by the MIP results.

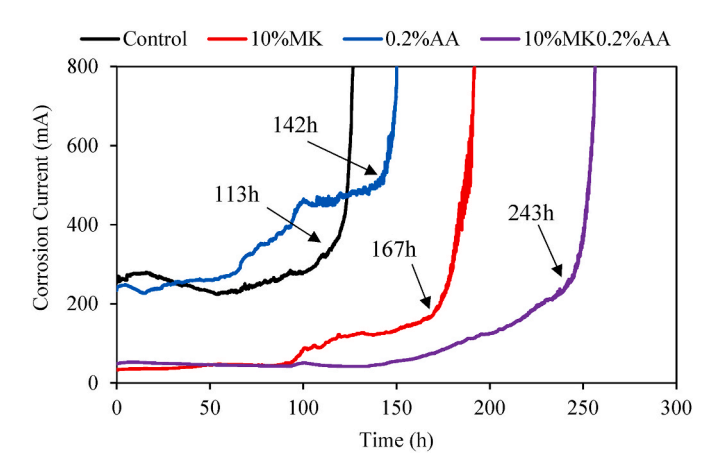


Fig. 14. Corrosion currents of reinforcing bars in four mortar samples.

In comparison to the control sample, the sample with 0.2 % AA initially shows a higher corrosion current after a few hours of testing due to its higher permeability resulting from the lower degree of hydration, as indicated by Table 3. However, its corrosion time is 25.6 % longer than the control sample, suggesting that the addition of AA can enhance the corrosion resistance of rebar. Similar effects of AA on the corrosion of rebar can also be observed in the two samples with MK. The use of AA in the MK blended mortar resulted in up to a 45.5 % improvement in corrosion time. The increased corrosion time may be attributed to the corrosion-inhibiting ability of AA, as well as the improved microstructure and mechanical properties induced by AA. Further study is needed to elucidate the respective roles of these factors in improving the corrosion resistance of rebars.

4. Conclusions

This study investigates the potential of AA, a naturally occurring chemical compound, as a multi-purpose admixture for MK blended mortar. AA can enhance several important properties of cement and MK blended mortars. Firstly, AA can act as a cement retarder, but high dosages (over 0.4 %) should be avoided to prevent excessive retardation. Secondly, AA can be used as a water reducer, promoting the dispersion of cement particles and improving the flowability of mortars. Thirdly, AA can enhance the compressive strength of cement and MK blended mortars, with a 0.2 % addition resulting in a 31 % increase in late-age compressive strength. This is attributed to AA's ability to lower porosity and increase the elastic modulus of the mortar. Fourthly, AA can reduce autogenous shrinkage in cement and MK blended mortars by up to 48 % due to its ability to reduce capillary pores smaller than 50 nm. Finally, AA can act as a corrosion inhibitor for rebars in concrete, increasing corrosion time and improving microstructure and mechanical properties.

Using AA as an admixture for mortar and concrete is an attractive option due to its renewable nature, eco-friendliness, and versatility. The addition of AA at a low dose of 0.2 % can significantly enhance late-age compressive strength, reducing the amount of cement needed and thus decreasing the carbon footprint of concrete/mortar production. Compared with commonly used retarder such as SG, AA possesses more functions and are more effective in enhancing the late-age strength of

the mortar. This study provides a viable approach to decarbonize concrete through enhancing the efficiency of the binder with a renewable chemical compound. Nevertheless, AA needs to be used with reactive powder to mitigate its retarding effect. The dosage of AA must be limited for the same reason.

CRediT authorship contribution statement

Liang Wang: Formal analysis, Methodology, Writing – original draft. Jialai Wang: Conceptualization, Formal analysis, Funding acquisition, Methodology, Project administration, Resources, Supervision, Writing – review & editing. Hao Wang: Data curation, Investigation. Xin Qian: Data curation, Investigation. Yi Fang: Investigation. Yan Ge: Investigation. Xuepeng Wang: Investigation. Xiaozhi Zhao: Investigation. Monica Lages Do Amaral: Investigation.

Declaration of competing interest

The authors declare that they have no known competing financial interests or personal relationships that could have appeared to influence the work reported in this paper.

Data availability

Data will be made available on request.

Acknowledgments

This work was supported by the Natural Science Research Project of Anhui Educational Committee (2023AH040156), National Natural Science Foundation of China (52108187), National Science Foundation – United States (1761672 and 2236331), Anhui Provincial Natural Science Foundation (2008085QE244), China Postdoctoral Science Foundation (2020M681988) and Anhui Provincial Key Research and Development Project (201904a07020081).

References

- [1] UNEP Copenhagen Climate Centre, Emissions Gap Report 2020, 2020.
- [2] U.N. Environment, K.L. Scrivener, V.M. John, E.M. Gartner, Eco-efficient cements: potential economically viable solutions for a low-CO2 cement-based materials industry, Cement Concr. Res. 114 (2018) 2–26.
- [3] B.B. Sabir, S. Wild, J. Bai, Metakaolin and calcined clays as pozzolans for concrete: a review, Cem. Concr. Compos. 23 (2001) 441–454.
- [4] P. Mikhailenko, F. Cassagnabère, A. Emam, M. Lachemi, Influence of physicochemical characteristics on the carbonation of cement paste at high replacement rates of metakaolin, Construct. Build. Mater. 158 (2018) 164–172.
- [5] J. Pera, Metakaolin and calcined clays, Cem. Concr. Compos. 6 (2001) iii.
- [6] S. Dadsetan, J. Bai, Mechanical and microstructural properties of self-compacting concrete blended with metakaolin, ground granulated blast-furnace slag and fly ash, Construct. Build. Mater. 146 (2017) 658–667.
- [7] G. Medjigbodo, E. Rozière, K. Charrier, L. Izoret, A. Loukili, Hydration, shrinkage, and durability of ternary binders containing Portland cement, limestone filler and metakaolin, Construct. Build. Mater. 183 (2018) 114–126.
- [8] Z. Mo, X. Gao, A. Su, Mechanical performances and microstructures of metakaolin contained UHPC matrix under steam curing conditions, Construct. Build. Mater. 268 (2021), 121112.
- [9] V.V. Praveen Kumar, N. Prasad, S. Dey, Influence of metakaolin on strength and durability characteristics of ground granulated blast furnace slag based geopolymer concrete, Struct. Concr. 21 (2020) 1040–1050.
- [10] A.A. Raheem, R. Abdulwahab, M.A. Kareem, Incorporation of metakaolin and nanosilica in blended cement mortar and concrete-A review, J. Clean. Prod. (2021), 125852.
- [11] A. Tafraoui, G. Escadeillas, S. Lebaili, T. Vidal, Metakaolin in the formulation of UHPC, Construct. Build. Mater. 23 (2009) 669–674.
- [12] Z. Li, Z. Ding, Property improvement of Portland cement by incorporating with metakaolin and slag, Cement Concr. Res. 33 (2003) 579–584.
- [13] P. Liu, The Research on the Clean Production Technique of Naphthalene Series Superplasticizer(master Dissertation), Xi'an University of Architecture and Technology, 2012.
- [14] N. Kovalchuk, J. Kelty, L. Li, M. Hartog, Q.-Y. Zhang, P. Edwards, L. Van Winkle, X. Ding, Impact of hepatic P450-mediated biotransformation on the disposition and

- respiratory tract toxicity of inhaled naphthalene, Toxicol. Appl. Pharmacol. 329(2017) 1-8.
- [15] G. Lai, X. Liu, S. Li, Y. Xu, Y. Zheng, J. Guan, R. Gao, Z. Wei, Z. Wang, S. Cui, Development of chemical admixtures for green and environmentally friendly concrete: a review, J. Clean. Prod. 389 (2023), 136116.
- [16] P. Chen, L. Zhang, J. Wang, X. Lou, L. Huang, Y. Xu, Exploring vitamin-C as a retarder for calcium sulfoaluminate cement, Construct. Build. Mater. 312 (2021), 125334.
- [17] K.M. Phillips, M.T. Tarrago-Trani, S.E. Gebhardt, J. Exler, K.Y. Patterson, D. B. Haytowitz, P.R. Pehrsson, J.M. Holden, Stability of vitamin C in frozen raw fruit and vegetable homogenates, J. Food Compos. Anal. 23 (2010) 253–259.
- [18] S. Ghafoor, R. Arain, K. Yasmeen, F. Ahmed, I. Saeed, Determination of ascorbic acid content of some capsicum cultivars by cyclic voltammetry performed at GCE by external standard series calibration method, Int. J. Electrochem. Sci. 9 (2014) 5751–5762
- [19] Sunwarrior, Natural vitamin C verses synthetic vitamin C, https://sunwarrior.com/blogs/health-hub/natural-vitamin-c-verses-synthetic-vitamin-c..
- [20] K. Herbers, Vitamin production in transgenic plants, J. Plant Physiol. 160 (2003) 821–829.
- [21] J. Zhou, G. Du, J. Chen, Metabolic engineering of microorganisms for vitamin C production, Reprogramming Microb, Metab. Pathways. 64 (2012) 241–259.
- [22] A. Anejjar, O.I. El Mouden, A. Batah, A. Bouskri, A. Rjoub, Corrosion inhibition potential of ascorbic acid on carbon steel in acid media, Appl. J. Environ. Eng. Sci. 3 (2017) 1–3.
- [23] N.K. Brixi, L. Sail, A. Bezzar, Application of ascorbic acid as green corrosion inhibitor of reinforced steel in concrete pore solutions contaminated with chlorides, J. Adhes. Sci. Technol. (2021) 1–24.
- [24] R. Fuchs-Godec, M. Pavlović, M. V Tomić, The inhibitive effect of vitamin-C on the corrosive performance of steel in HCl solutions-part II, Int. J. Electrochem. Sci. 10 (2015) 10502–10512.
- [25] I. Erel-Unal, S.A. Sukhishvili, Hydrogen-bonded multilayers of a neutral polymer and a polyphenol, Macromolecules 41 (2008) 3962–3970.
- [26] M. Andjelković, J. Van Camp, B. De Meulenaer, G. Depaemelaere, C. Socaciu, M. Verloo, R. Verhe, Iron-chelation properties of phenolic acids bearing catechol and galloyl groups, Food Chem. 98 (2006) 23–31.
- [27] Q. Xu, D. Hou, H. Zhang, P. Wang, M. Wang, D. Wu, C. Liu, Z. Ding, M. Zhang, Z. Xin, B. Fu, J. Guan, Y. Zhang, Understanding the effect of vitamin B3, B6 and C as a corrosion inhibitor on the ordinary Portland cement hydration: experiments and DFT study, Construct. Build. Mater. 331 (2022), 127294.
- [28] C. Argiz, C. Arroyo, A. Bravo, A. Moragues, C. Andrade, F.M. Bolzoni, L-ascorbic acid as an efficient green corrosion inhibitor of steel rebars in chloride contaminated cement mortar, Materials 15 (2022) 8005.
- [29] ASTM C1437, Standard Test Method for Flow of Hydraulic Cement Mortar, ASTM International, West Conshohocken, PA, USA, 2020.
- [30] ASTM C1702-17, Standard Test Method for Measurement of Heat of Hydration of Hydraulic Cementitious Materials Using Isothermal Conduction Calorimetry, ASTM International, West Conshohocken, PA, 2017.
- [31] A. Machner, M. Zajac, M. Ben, K.O. Kjellsen, M.R. Geiker, Chloride-binding capacity of hydrotalcite in cement pastes containing dolomite and metakaolin, Cement Concr. Res. 107 (2018) 163–181.
- [32] Y. Chen, C.R. Rodriguez, Z. Li, B. Chen, O. Çopuroğlu, E. Schlangen, Effect of different grade levels of calcined clays on fresh and hardened properties of ternaryblended cementitious materials for 3D printing, Cem. Concr. Compos. 114 (2020), 103708.
- [33] P. Monda, Nanomechanical Properties of Cementitious Materials, Northwestern University, 2018.
- [34] W.C. Oliver, G.M. Pharr, Measurement of hardness and elastic modulus by instrumented indentation: advances in understanding and refinements to methodology, J. Mater. Res. 19 (2004) 3–20.
- [35] R.J. Pellenq, A. Kushima, R. Shahsavari, K.J. Van Vliet, M.J. Buehler, S. Yip, F.-J. Ulm, A realistic molecular model of cement hydrates, Proc. Natl. Acad. Sci. USA 106 (2009) 16102–16107.
- [36] ASTM C1698, Standard Test Method for Autogenous Strain of Cement Paste and Mortar, ASTM International, West Conshohocken, PA, USA, 2019.
- [37] E. Güneyisi, T. Özturan, M. Gesoğlu, A study on reinforcement corrosion and related properties of plain and blended cement concretes under different curing conditions, Cem. Concr. Compos. 27 (2005) 449–461.
- [38] S. Çınar, M. Akinc, Ascorbic acid as a dispersant for concentrated alumina nanopowder suspensions, J. Eur. Ceram. Soc. 34 (2014) 1997–2004.
- [39] M. Antoni, J. Rossen, F. Martirena, K. Scrivener, Cement substitution by a combination of metakaolin and limestone, Cement Concr. Res. 42 (2012) 1579–1589.
- [40] Y. Fang, J. Wang, L. Wang, X. Qian, X. Wang, W. Liao, P. Chen, H. Ma, Densifying hydration products of alite by a bio-inspired admixture, Mater. Des. 225 (2023) 111490.
- [41] Z. Wu, H. Lian, High Performance Concrete, China Railway Press, Beijing, China,
- [42] Y. Li, J. Bao, Y. Guo, The relationship between autogenous shrinkage and pore structure of cement paste with mineral admixtures, Construct. Build. Mater. 24 (2010) 1855–1860.
- [43] N. Perez, Electrochemistry and Corrosion Science, Springer, 2004.